

DisC-VC: Disentangled and F_0 -Controllable Neural Voice Conversion

Chihiro Watanabe^{*1} and Hirokazu Kameoka^{†1}

¹NTT Communication Science Laboratories, 3-1, Morinosato Wakamiya, Atsugi-shi, Kanagawa Pref. 243-0198 Japan

Abstract

Voice conversion is a task to convert a non-linguistic feature of a given utterance. Since naturalness of speech strongly depends on its pitch pattern, in some applications, it would be desirable to keep the original rise/fall pitch pattern while changing the speaker identity. Some of the existing methods address this problem by either using a source-filter model or developing a neural network that takes an F_0 pattern as input to the model. Although the latter approach can achieve relatively high sound quality compared to the former one, there is no consideration for discrepancy between the target and generated F_0 patterns in its training process. In this paper, we propose a new variational-autoencoder-based voice conversion model accompanied by an auxiliary network, which ensures that the conversion result correctly reflects the specified F_0 /timbre information. We show the effectiveness of the proposed method by objective and subjective evaluations.

Keywords. Voice conversion, F_0 conversion, timbre conversion, neural network, variational autoencoder

1 Introduction

Voice conversion (VC) is a task to convert a non-linguistic feature of a given utterance and it can be used for various applications [24] including personalizing or changing emotion of text-to-speech systems [8, 11, 31]. In this paper, we focus on the conversion of F_0 pattern and timbre (i.e., speaker identity).

A basic VC framework consists of feature extraction from a speech signal, feature conversion, and speech synthesis based on a converted feature. With regard to feature conversion, some of the existing methods require parallel data set (e.g., Gaussian-mixture-model-based [10, 35, 38], deep-neural-network-based [3, 4], and sequence-to-sequence-based [30, 41] methods), while others do not (e.g., recognition-synthesis-based [7, 21], phonetic-posteriorgram-based [36], variational-autoencoder (VAE) [18]-based [12, 28, 29], generative-adversarial-network-based [6, 15, 16], flow-based [23, 34], and score-based [13, 26] methods). As for feature extraction and speech synthesis, the existing methods can be classified roughly into two approaches. One is the parametric-vocoder-based (PV) approach [4, 12, 35], where we first apply timbre conversion based on mel-cepstral coefficients (MCCs) and F_0 conversion (e.g., linear transformation) separately and then synthesize a waveform with a parametric vocoder such as WORLD [25]. The other is the neural-vocoder-based (NV) approach [2, 14, 29], where we use a neural network for speech synthesis. While early neural vocoders have required spectral envelope- and excitation-related features as input [5, 37], the recent mainstream is to synthesize a waveform from a mel-spectrogram [20, 40].

^{*}chihiro.watanabe.xz@hco.ntt.co.jp

[†]This work was supported by JST CREST Grant Number JPMJCR19A3, Japan.

In some applications such as online communication, it would be desirable to keep the original rise/fall pitch pattern, since it strongly affects the nuance of speech. Inappropriate modification of the relative pitch pattern would cause miscommunication in regard to the speaker’s intent and/or emotion. One way to securely keep the relative pitch pattern of input speech would be to take the PV approach, which allows us to explicitly specify the F_0 pattern of the converted speech. However, one disadvantage is that it cannot generally achieve as high sound quality as the NV approach. Recently, some F_0 -controllable NV methods have been proposed, with which we can specify both F_0 and timbre conditionings explicitly [17, 22, 27]. However, even with these models, a generated speech does not necessarily have the same F_0 pattern as the input conditioning. This is because the relationship between the specified F_0 pattern and the conversion result has not been considered in the training criteria, and thus the decoder may disregard the specified F_0 pattern and not reproduce it faithfully in the reconstruction process.

In this paper, we develop a disentangled and F_0 -controllable neural VC (DisC-VC). DisC consists of the VAE-based generator and auxiliary network. The auxiliary network, which is composed of F_0 extractor and speaker classifier, ensures that the conversion result correctly reflects the specified F_0 /timbre information. We show the effectiveness of DisC by both objective and subjective evaluations.

2 Proposed Method

2.1 Preprocessing of training samples

Figure 1 shows the architecture of the DisC model. During the training phase, we use the standardized log mel-spectrogram $\mathbf{x} \in \mathbb{R}^{F \times T}$, the log F_0 pattern $\boldsymbol{\lambda} \in \mathbb{R}^T$, and the speaker index $s \in \{1, 2, \dots, S\}$ as the input features, where T , F , and S indicate the numbers of time and frequency bins and speakers, respectively. To define \mathbf{x} , we first compute the log mel-spectrogram $\mathbf{x}^{(0)}$. Then, each entry of the column vectors of $\mathbf{x}^{(0)}$ is standardized according to the mean and standard deviation for all the time bins and training samples. To compute $\boldsymbol{\lambda}$, we extract the F_0 pattern from an input speech signal with the WORLD F_0 estimator [25] and apply logarithmic transformation to its non-zero entries.

2.2 Generator

The generator consists of content encoder ENC_C and decoder DEC. To reflect the discrete nature of the phonemic units of speech, we adopt the encoder of Vector Quantised-Variational AutoEncoder or VQ-VAE [39] as ENC_C . In the generator, we first extract the content feature $\mathbf{c} = \text{ENC}_C(\mathbf{x}) \in \mathbb{R}^{N_C \times T}$ from \mathbf{x} , where we set $N_C = 16$ in the experiment. Then, the decoder reconstructs the mean and variance of the log mel-spectrogram $(\hat{\boldsymbol{\mu}}, \hat{\boldsymbol{\sigma}}) = \text{DEC}(\mathbf{c}, \boldsymbol{\lambda}, s)$, where $\hat{\boldsymbol{\mu}}, \hat{\boldsymbol{\sigma}} \in \mathbb{R}^{F \times T}$.

2.3 Training objective

2.3.1 Reconstruction error

The first training objective is the reconstruction error of the generator. Let $q_\phi(\mathbf{c}|\mathbf{x})$ be a probability density function (PDF) of content feature \mathbf{c} conditioned on log mel-spectrogram \mathbf{x} , based on which the content encoder with parameter ϕ generates the content feature. Let $p_\theta(\mathbf{x}|\mathbf{c}, \boldsymbol{\lambda}, s)$ be a PDF of \mathbf{x} conditioned on a set of features $(\boldsymbol{\lambda}, s)$, based on which the decoder with parameter θ generates the output mel-spectrogram. We assume the prior distribution of \mathbf{c} to be a discrete uniform distribution independent of the F_0 /timbre features (i.e., $p(\mathbf{c}|\boldsymbol{\lambda}, s) = p(\mathbf{c})$). By using Jensen’s inequality, the negative log marginal distribution can be upper bounded by

$$-\log p_\theta(\mathbf{x}|\boldsymbol{\lambda}, s) \leq D - \mathbb{E}_{\mathbf{c} \sim q_\phi(\mathbf{c}|\mathbf{x})}[\log p_\theta(\mathbf{x}|\mathbf{c}, \boldsymbol{\lambda}, s)], \quad (1)$$

where $D := D_{\text{KL}}[q_\phi(\mathbf{c}|\mathbf{x})||p(\mathbf{c})]$ and $D_{\text{KL}}(q||p)$ indicates the KL divergence of q from p . It can be shown that the difference between the right- and left-hand sides of (1) is equal to $D_{\text{KL}}(q_\phi(\mathbf{c}|\mathbf{x})||p_\theta(\mathbf{c}|\mathbf{x}, \boldsymbol{\lambda}, s))$,

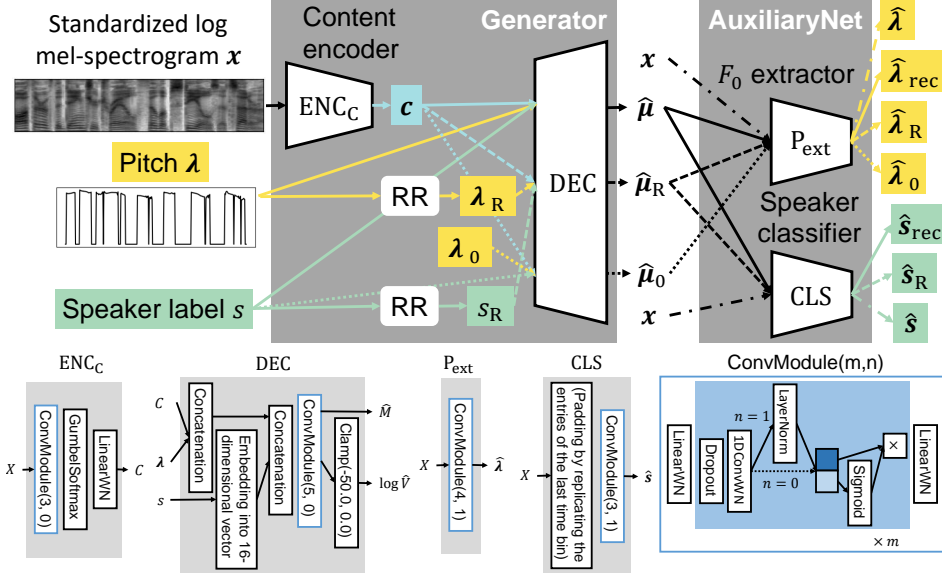


Figure 1: The network architecture of the DisC-VC. ‘‘GumbelSoftmax’’ means sampling from the Gumbel-Softmax distribution [9]. ‘‘LinearWN’’ and ‘‘1DConvWN,’’ respectively, are linear and 1D convolution layers with weight normalization [32]. Clamp(a, b) is a function that clamps input into the range $[a, b]$. ‘‘LayerNorm’’ means layer normalization [1].

which is minimized when $q_\phi(c|\mathbf{x}) = p_\theta(c|\mathbf{x}, \boldsymbol{\lambda}, s)$ (i.e., the content feature c extracted by the encoder is independent of $(\boldsymbol{\lambda}, s)$, given \mathbf{x}). When $p(c)$ is a discrete uniform distribution, D becomes constant [39]. By assuming $p_\theta(\mathbf{x}|c, \boldsymbol{\lambda}, s)$ to be a Gaussian distribution with mean $\hat{\boldsymbol{\mu}}$ and variance $\hat{\boldsymbol{\sigma}}$, where all the entries are mutually independent, the second term in (1) can be interpreted as the reconstruction error of \mathbf{x} . Given training samples of $(\mathbf{x}, \boldsymbol{\lambda}, s)$, the actual training criterion $\mathcal{L}_{\text{like}}$ will be the expectation of the right-hand side of (1) over $(\mathbf{x}, \boldsymbol{\lambda}, s)$.

2.3.2 Negative mutual information

As we later show experimentally in Section 3, even if the conversion model is conditioned on specified F_0 /timbre information $(\boldsymbol{\lambda}_R, s_R)$, the converted speech does not always reflect them sufficiently with a model trained only based on the reconstruction loss $\mathcal{L}_{\text{like}}$, since the decoder may disregard $(\boldsymbol{\lambda}_R, s_R)$ and only use c to reconstruct the log mel-spectrogram. Therefore, as the second training objective, given $c \sim q_\phi(c|\mathbf{x})$ and s_R , we consider the negative mutual information $\mathcal{I}_P(\boldsymbol{\theta})$ between output log mel-spectrogram $\mathbf{x} \sim p_\theta(\mathbf{x}|c, \boldsymbol{\lambda}_R, s_R)$ and $\boldsymbol{\lambda}_R$, which is given by

$$\mathcal{I}_P(\boldsymbol{\theta}) = -\mathbb{E}_{\mathbf{x} \sim p_\theta(\mathbf{x}|c, \boldsymbol{\lambda}_R, s_R), \boldsymbol{\lambda}'_R \sim p(\boldsymbol{\lambda}'_R|\mathbf{x})} [\log p(\boldsymbol{\lambda}'_R|\mathbf{x})] + H_P, \quad (2)$$

where $H_P := \mathbb{E}_{\boldsymbol{\lambda}_R \sim p(\boldsymbol{\lambda}_R)} [\log p(\boldsymbol{\lambda}_R)]$ is a constant that does not depend on $\boldsymbol{\theta}$. By using the fact that a KL divergence is non-negative and the law of total expectation, the expectation of the first term in (2) over $\boldsymbol{\lambda}_R$ can be upper bounded by

$$\begin{aligned} & -\mathbb{E}_{\boldsymbol{\lambda}_R \sim p(\boldsymbol{\lambda}_R), \mathbf{x} \sim p_\theta(\mathbf{x}|c, \boldsymbol{\lambda}_R, s_R), \boldsymbol{\lambda}'_R \sim p(\boldsymbol{\lambda}'_R|\mathbf{x})} [\log p(\boldsymbol{\lambda}'_R|\mathbf{x})] \\ & \leq -\mathbb{E}_{\boldsymbol{\lambda}_R \sim p(\boldsymbol{\lambda}_R), \mathbf{x} \sim p_\theta(\mathbf{x}|c, \boldsymbol{\lambda}_R, s_R), \boldsymbol{\lambda}'_R \sim p(\boldsymbol{\lambda}'_R|\mathbf{x})} [\log q(\boldsymbol{\lambda}'_R|\mathbf{x})] \\ & = -\mathbb{E}_{\boldsymbol{\lambda}_R \sim p(\boldsymbol{\lambda}_R), \mathbf{x} \sim p_\theta(\mathbf{x}|c, \boldsymbol{\lambda}_R, s_R)} [\log q(\boldsymbol{\lambda}_R|\mathbf{x})] =: R_P, \end{aligned} \quad (3)$$

where $q(\boldsymbol{\lambda}'_R|\mathbf{x})$ is an arbitrary conditional PDF. The equality holds if $q(\boldsymbol{\lambda}'_R|\mathbf{x}) = p(\boldsymbol{\lambda}'_R|\mathbf{x})$. Therefore, assuming $q(\boldsymbol{\lambda}'_R|\mathbf{x})$ in some parametric form, the left-hand side of (3) can be decreased by alternately

decreasing R_P with respect to (ϕ, θ) and q . Specifically, for all $i \in \{1, \dots, T\}$, we represent $q((\lambda_R)_i | \mathbf{x})$ as the Laplace distribution with location parameter $(\hat{\lambda}_R)_i$ and scale parameter of one, where $\hat{\lambda}_R = P_{\text{ext}}(\hat{\mu}_R)$ is an output of an auxiliary neural network (i.e., F_0 extractor) $P_{\text{ext}} : \mathbb{R}^{F \times T} \mapsto \mathbb{R}^T$ and $(\hat{\mu}_R, \hat{\sigma}_R) = \text{DEC}(C, \lambda_R, s_R)$, and consider training its parameters ψ_P along with ϕ and θ . Hence, P_{ext} is trained to estimate the log F_0 pattern from an input log mel-spectrogram.

Given \mathbf{c} and λ_R , we also consider using the negative mutual information $\mathcal{I}_T(\theta)$ between \mathbf{x} and s_R as a training criterion. As above, the expectation of $\mathcal{I}_T(\theta)$ except for a constant term over s_R can be upper bounded by $R_T := -\mathbb{E}_{s_R \sim p(s_R), \mathbf{x} \sim p_\theta(\mathbf{x} | \mathbf{c}, \lambda_R, s_R)}[\log r(s_R | \mathbf{x})]$, where $r(s_R | \mathbf{x})$ is an arbitrary categorical distribution and the exact bound is achieved when $r(s_R | \mathbf{x}) = p(s_R | \mathbf{x})$. Thus, it can be decreased by alternately decreasing R_T with respect to r and (ϕ, θ) . Here, we assume $r(s_R | \mathbf{x})$ to be a categorical distribution with each probability given as an output of an auxiliary neural network (i.e., speaker classifier) $\text{CLS} : \mathbb{R}^{F \times T} \mapsto \mathbb{R}^{T_S}$ ¹, and consider training its parameters ψ_T along with ϕ , θ , and ψ_P . Hence, CLS is trained to detect the speaker from an input log mel-spectrogram.

The criteria R_P and R_T are defined under specific (\mathbf{c}, s_R) and (\mathbf{c}, λ_R) , respectively. Since \mathbf{c} , s_R , and λ_R are determined stochastically according to the training examples, the actual criteria used for training will be the expectations of R_P and R_T with respect to \mathbf{c} , s_R , and λ_R . Let $\mathcal{L}_P := \mathbb{E}_{\mathbf{x}' \sim p(\mathbf{x}'), \mathbf{c} \sim q_\phi(\mathbf{c} | \mathbf{x}'), s_R \sim p(s_R)}[R_P]$ and $\mathcal{L}_T := \mathbb{E}_{\mathbf{x}' \sim p(\mathbf{x}'), \mathbf{c} \sim q_\phi(\mathbf{c} | \mathbf{x}'), \lambda_R \sim p(\lambda_R)}[R_T]$, where $\mathbf{x}' \sim p(\mathbf{x}')$ indicates the log mel-spectrogram of a randomly drawn training sample. The process $\lambda_R \sim p(\lambda_R)$ can be implemented as random resampling (RR), which converts an input log F_0 pattern λ into random one λ_R . In the experiment, we defined the RR of F_0 by $(\lambda_R)_i = \lambda_i + \beta$ with $\beta \sim \text{Uniform}([0.3, 3])$, if $\lambda_i \neq 0$, and $(\lambda_R)_i = \lambda_i$, otherwise. We also defined the RR of speaker index by generating s_R from a discrete uniform distribution on $\{1, \dots, S\}$. The idea of RR has also been adopted in SpeechFlow [28], however, there has been no consideration for the discrepancy between the specified F_0 /timbre information and those of the conversion result.

The actual flow of computing \mathcal{L}_P and \mathcal{L}_T can be explained as follows. For each training sample \mathbf{x}' , the decoder generates \mathbf{x} using $\mathbf{c} = \text{ENC}_C(\mathbf{x}')$ along with λ_R and s_R randomly drawn from predefined distributions $p(\lambda_R)$ and $p(s_R)$, respectively. The auxiliary network then extracts $\hat{\lambda}_R$ and \hat{s}_R from \mathbf{x} and checks whether they are consistent with λ_R and s_R . In addition, to better express unvoiced and voiced speech differently, we define \mathcal{L}_{P0} for a zero vector $\lambda_0 \in \mathbb{R}^T$ and $\hat{\lambda}_0 = P_{\text{ext}}(\hat{\mu}_0)$ as a training criterion, where $(\hat{\mu}_0, \hat{\sigma}_0) = \text{DEC}(C, \lambda_0, s)$. We also define \mathcal{L}_{P1} for λ and $\hat{\lambda} = P_{\text{ext}}(\hat{\mu})$, \mathcal{L}_{P2} for λ and $\hat{\lambda}_{\text{rec}} = P_{\text{ext}}(\hat{\mu})$, \mathcal{L}_{T1} for s and $\hat{s} = \text{CLS}(\mathbf{x})$, and \mathcal{L}_{T2} for s and $\hat{s}_{\text{rec}} = \text{CLS}(\hat{\mu})$.

We train the entire network to minimize $\mathcal{L} := \eta \mathcal{L}_{\text{like}} + \eta_P (\mathcal{L}_P + \mathcal{L}_{P0} + \mathcal{L}_{P1} + \mathcal{L}_{P2}) + \eta_T (\mathcal{L}_T + \frac{1}{2} \mathcal{L}_{T1} + \frac{1}{2} \mathcal{L}_{T2})$ based on back-propagation. In the experiment, we set $\eta = 1/FT$, $\eta_P = 1/4T$, and $\eta_T = 1/2T_S$, and replaced expectation over \mathbf{x}' in computing each loss with a sample mean of a given mini-batch, which consists of 16 randomly selected training samples. A training sample was defined as $\{(\mathbf{x}_s, \lambda_s, s) | s = 1, \dots, S\}$, where \mathbf{x}_s and λ_s were a log mel-spectrogram and a log F_0 pattern of the s th speaker, respectively. It must be noted that the criterion \mathcal{L} can be used not only for training the generator considered in this study, but also for training other existing generator networks that allow F_0 /timbre conditioning (e.g., SpeechFlow [28]).

2.4 Conversion Process

By using the trained DisC model, we can apply the following types of conversion to a given test sample (\mathbf{x}, λ, s) : (1) change log F_0 pattern by a given value $\beta \in \mathbb{R}$, (2) change log F_0 pattern from speaker s to \check{s}_P , and (3) change timbre from speaker s to \check{s}_T . By defining $\beta = 0$, $\check{s}_P = s$, or $\check{s}_T = s$, we can also perform each type of conversion individually.

The target log F_0 pattern $\check{\lambda} \in \mathbb{R}^T$ is defined as follows. Let $\mu_P(s)$ and $\sigma_P(s)$, respectively, be the sample mean and sample standard deviation of the log F_0 pattern (except for the zero entries) of the s th speaker in the training data set. For all $i \in \{1, \dots, T\}$, we define $\check{\lambda}_i = [\sigma_P(\check{s}_P)/\sigma_P(s)][\lambda_i - \mu_P(s)] +$

¹ T_S is an arbitrary natural number. As shown in Figure 1, CLS contains convolutional layers and thus T_S depends on T in the experiment.

$\mu_P(\check{s}_P) + \beta$, if $\lambda_i \neq 0$, and $\check{\lambda}_i = 0$, otherwise.

We obtain $(\hat{\mu}, \hat{\sigma}) = \text{DEC}(\text{ENC}_C(\mathbf{x}), \check{\lambda}, \check{s}_T)$ and reconstruct a waveform from $\hat{\mu}$ with a neural vocoder. In the experiment, we used Parallel WaveGAN [40].

3 Experiment

3.1 Experimental settings

By using the CMU Arctic speech databases [19], we trained the DisC model with the 1,000 training samples per speaker for 5,000 epochs, applied F_0 and/or timbre conversion to the 132 test samples per speaker, and compared the results with those obtained with the following baseline methods.

DisC-NoAux is DisC with no auxiliary network, and it is trained by minimizing $\mathcal{L}_{\text{like}}$ in Section 2.3.1. ACVAE-C [12] is the original ACVAE that takes MCCs as input and reconstructs a waveform from converted MCCs and F_0 pattern by using a WORLD vocoder [25]. ACVAE-S [14] is the extended ACVAE that takes mel-spectrogram as input and reconstructs a waveform from a converted mel-spectrogram by using a neural vocoder. For reference, we also used WORLD vocoder [25] itself for F_0 -only conversion by using the MCCs of an input signal and $\check{\lambda}$ given in Section 2.4. We also tried F_0 and timbre conversion with BNE-Seq2seqMoL (BNE) [22] as an example of F_0 -controllable methods. It must be noted that we cannot compare its result with those of the other methods as it is, since we used the pretrained synthesis model provided by the authors of [22], which was trained with a different data set than the CMU Arctic one.

To compare these methods, we tried **task P** to change $\log F_0$ pattern by $\beta \in \{\log(1.5), -\log(1.5)\}$, **task T** to change timbre to that of a target speaker, and **task PT** to change both F_0 pattern and timbre to those of a target speaker. Since only simultaneous conversion of F_0 pattern and timbre is possible with ACVAE-S, we use the same results in tasks T and PT for this method. Before evaluation, we trimmed the leading and trailing silent sections of all the target and converted samples.

3.2 Objective evaluation

To evaluate F_0 and timbre conversion performance, we adopted the F_0 error ΔF_0 (i.e., the root mean squared error between two $\log F_0$ patterns) and the mel-cepstral distortion (MCD), respectively. Since target and converted speech signals are not necessarily aligned in the time direction, we first applied endpoint-free Dynamic Time Warping to a given pair of $\log F_0$ patterns or MCCs and then computed ΔF_0 and the MCD with the optimally aligned sequences. For all the tasks, we computed ΔF_0 between the target $\log F_0$ pattern $\check{\lambda}$ and that of the converted speech. We evaluated the MCD between the samples before and after conversion for task P and those between the target and converted samples for tasks T and PT.

Tables 1, 2, and 3 show the results of tasks P, T, and PT, respectively. Table 1 shows that the timbre of the source speech was maintained more successfully with DisC than with DisC-NoAux in F_0 -only conversion. In the same task, we also see that the F_0 conversion performance of DisC was better than that of DisC-NoAux. Tables 2 and 3 show that timbre conversion was more successfully done by DisC than by ACVAE-C, whereas F_0 conversion was more successfully done by DisC than by ACVAE-S (especially in timbre-only conversion task). ACVAE-C and -S achieved the best performance in terms of ΔF_0 and the MCD, respectively, however, they could not keep these criteria small at the same time.

3.3 Subjective evaluation

To conduct subjective evaluation, we randomly chose three test samples for each of the quality and timbre evaluations and for each setting (i.e., a combination of β , a source speaker, and a conversion method in task T and a combination of a source and target speakers and a conversion method in tasks T and PT). For timbre evaluation, we concatenated target and converted speech samples with a 1 s

Table 1: MCD from a source speaker and F_0 error ΔF_0 in task P. The values before and after \pm , respectively, indicate the mean and the standard deviation for all the settings and test samples.

	DisC	DisC-NoAux	(WORLD)
MCD	6.14 ± 0.37	6.33 ± 0.47	4.23 ± 1.11
ΔF_0	0.22 ± 0.10	0.24 ± 0.11	0.14 ± 0.12

Table 2: MCD from a target speaker and ΔF_0 in task T.

	DisC	DisC-NoAux	ACVAE-C	ACVAE-S
MCD	7.29 ± 0.74	7.33 ± 0.78	7.62 ± 0.73	6.65 ± 0.68
ΔF_0	0.24 ± 0.14	0.30 ± 0.20	0.12 ± 0.11	0.36 ± 0.18

Table 3: MCD from a target speaker and ΔF_0 in task PT.

	DisC	DisC-NoAux	ACVAE-C	ACVAE-S	(BNE)
MCD	6.83 ± 0.63	6.80 ± 0.63	7.62 ± 0.74	6.65 ± 0.68	7.81 ± 0.67
ΔF_0	0.13 ± 0.11	0.14 ± 0.11	0.12 ± 0.10	0.14 ± 0.10	0.19 ± 0.13

Table 4: MOS for sound quality. The values before and after \pm , respectively, indicate the mean and the standard deviation for all the listeners, settings, and selected test samples.

Task	DisC	DisC-NoAux	WORLD	ACVAE-C	ACVAE-S
P	2.62 ± 1.05	2.42 ± 1.12	2.95 ± 1.17	–	–
T	2.57 ± 1.15	2.42 ± 1.19	–	2.24 ± 0.98	3.55 ± 0.94
PT	3.45 ± 0.91	3.77 ± 0.89	–	2.36 ± 1.04	3.55 ± 0.94

Table 5: Score of ABX test for timbre similarity. Each value indicates similarity with source speakers for task P and that with target speakers for tasks T and PT.

Task	DisC	DisC-NoAux	WORLD	ACVAE-C	ACVAE-S
P	2.03 ± 0.83	1.85 ± 0.85	1.34 ± 0.59	–	–
T	2.06 ± 1.18	2.06 ± 1.10	–	1.59 ± 0.85	3.41 ± 0.69
PT	3.33 ± 0.80	3.37 ± 0.75	–	2.36 ± 0.88	3.41 ± 0.69

silent interval. We defined the target speech sample as a randomly selected one of the target speaker (i.e., the text content is not necessarily the same as that of the converted one). By considering the fact that we use the same result for tasks T and PT with regard to ACVAE-S, each of 15 listeners was presented 324 samples in each of quality and timbre evaluations.

We conducted a mean opinion score (MOS) test for sound quality, where each listener scores the sound quality of each sample by choosing one out of the five options, “1: Bad,” “2: Poor,” “3: Fair,” “4: Good,” and “5: Excellent.” Timbre evaluation was done based on the ABX test for speaker similarity, where he/she chooses one out of the four options, “1: Different (sure),” “2: Different (not sure),” “3: Same (not sure),” and “4: Same (sure),” for each concatenated sample.

Tables 4 and 5, respectively, show the results of the quality and timbre evaluations. In task P, F_0 conversion by WORLD vocoder achieved the best sound quality, however, DisC could maintain the timbre of the source speaker the best. When converting only timbre (i.e., task T), neither DisC nor DisC-NoAux could achieve as high sound quality and timbre maintenance as ACVAE-S. However, by converting F_0 pattern and timbre simultaneously (i.e., task PT), they could achieve comparable performance to ACVAE-S. A possible reason for this would be that speaker identity strongly depends on the average fundamental frequency, as also pointed out in [33].

4 Conclusion

We developed a new F_0 -controllable VC method DisC that takes into account discrepancy between the target and generated F_0 patterns in the training process. In this paper, we assumed that the same set of speakers appears in training and test data sets. It would be important to extend DisC so that it can be applied to unseen speakers in the test phase. Another future direction would be to take into account other prosody information (e.g., rhythm and stress) as controllable features.

References

- [1] J. L. Ba, J. R. Kiros, and G. E. Hinton. Layer normalization. In *NeurIPS 2016 Deep Learning Symposium*, 2016.
- [2] F. Biadsy, R. J. Weiss, P. J. Moreno, D. Kanvesky, and Y. Jia. Parrotron: An end-to-end speech-to-speech conversion model and its applications to hearing-impaired speech and speech separation. In *Interspeech*, pages 4115–4119, 2019.
- [3] S. Desai, A. W. Black, B. Yegnanarayana, and K. Prahallad. Spectral mapping using artificial neural networks for voice conversion. *TASLP*, 18(5):954–964, 2010.
- [4] S. Desai, E. V. Raghavendra, B. Yegnanarayana, A. W. Black, and K. Prahallad. Voice conversion using artificial neural networks. In *ICASSP*, pages 3893–3896, 2009.
- [5] T. Hayashi, A. Tamamori, K. Kobayashi, K. Takeda, and T. Toda. An investigation of multi-speaker training for wavenet vocoder. In *ASRU*, pages 712–718, 2017.
- [6] C.-C. Hsu, H.-T. Hwang, Y.-C. Wu, Y. Tsao, and H.-M. Wang. Voice conversion from unaligned corpora using variational autoencoding Wasserstein generative adversarial networks. In *Interspeech*, pages 3364–3368, 2017.
- [7] W.-C. Huang, Y.-C. Wu, and T. Hayashi. Any-to-one sequence-to-sequence voice conversion using self-supervised discrete speech representations. In *ICASSP*, pages 5944–5948, 2021.
- [8] Z. Inanoglu and S. Young. Data-driven emotion conversion in spoken English. *Speech Communication*, 51(3):268–283, 2009.
- [9] E. Jang, S. Gu, and B. Poole. Categorical reparameterization with Gumbel-Softmax. In *ICLR*, 2017.
- [10] A. Kain and M. W. Macon. Spectral voice conversion for text-to-speech synthesis. In *ICASSP*, pages 285–288, 1998.
- [11] A. Kain and M. W. Macon. Text-to-speech voice adaptation from sparse training data. In *ICSLP*, page paper 0902, 1998.
- [12] H. Kameoka, T. Kaneko, K. Tanaka, and N. Hojo. ACVAE-VC: Non-parallel voice conversion with auxiliary classifier variational autoencoder. *TASLP*, 27(9):1432–1443, 2019.
- [13] H. Kameoka, T. Kaneko, K. Tanaka, N. Hojo, and S. Seki. VoiceGrad: Non-parallel any-to-many voice conversion with annealed Langevin dynamics. arXiv:2010.02977, 2020.
- [14] H. Kameoka, T. Kaneko, K. Tanaka, and S. Seki. ACVAE-VC: Auxiliary classifier variational autoencoder voice conversion. <http://www.kecl.ntt.co.jp/people/kameoka.hirokazu/Demos/acvae-vc3/index.html>.
- [15] T. Kaneko and H. Kameoka. CycleGAN-VC: Non-parallel voice conversion using cycle-consistent adversarial networks. In *EUSIPCO*, pages 2100–2104, 2018.
- [16] T. Kaneko, H. Kameoka, K. Tanaka, and N. Hojo. StarGAN-VC2: Rethinking conditional methods for StarGAN-based voice conversion. In *Interspeech*, pages 679–683, 2019.
- [17] K.-W. Kim, S.-W. Park, J. Lee, and M.-C. Joe. ASSEM-VC: Realistic voice conversion by assembling modern speech synthesis techniques. In *ICASSP*, pages 6997–7001, 2022.
- [18] D. P. Kingma and M. Welling. Auto-encoding variational bayes. In *ICLR*, 2014.

- [19] J. Kominek and A. W. Black. The CMU Arctic speech databases. In *SSW5-2004*, pages 223–224, 2004.
- [20] J. Kong, J. Kim, and J. Bae. HiFi-GAN: Generative adversarial networks for efficient and high fidelity speech synthesis. In *NeurIPS*, volume 33, pages 17022–17033, 2020.
- [21] Y. Y. Lin, C.-M. Chien, J.-H. Lin, H. y. Lee, and L. s. Lee. Fragmentvc: Any-to-any voice conversion by end-to-end extracting and fusing fine-grained voice fragments with attention. In *ICASSP*, pages 5939–5943, 2021.
- [22] S. Liu, Y. Cao, D. Wang, X. Wu, X. Liu, and H. Meng. Any-to-many voice conversion with location-relative sequence-to-sequence modeling. *TASLP*, 29:1717–1728, 2021.
- [23] T. Merritt, A. Ezzerg, P. Biliński, M. Proszewska, K. Pokora, R. Barra-Chicote, and D. Korzekwa. Text-free non-parallel many-to-many voice conversion using normalising flow. In *ICASSP*, pages 6782–6786, 2022.
- [24] S. H. Mohammadi and A. Kain. An overview of voice conversion systems. *Speech Communication*, 88:65–82, 2017.
- [25] M. Morise, F. Yokomori, and K. Ozawa. WORLD: A vocoder-based high-quality speech synthesis system for real-time applications. *IEICE Transactions on Information and Systems*, E99.D(7):1877–1884, 2016.
- [26] V. Popov, I. Vovk, V. Gogoryan, T. Sadekova, M. S. Kudinov, and J. Wei. Diffusion-based voice conversion with fast maximum likelihood sampling scheme. In *ICLR*, 2022.
- [27] K. Qian, Z. Jin, M. Hasegawa-Johnson, and G. J. Mysore. F0-consistent many-to-many non-parallel voice conversion via conditional autoencoder. In *ICASSP*, pages 6284–6288, 2020.
- [28] K. Qian, Y. Zhang, S. Chang, M. Hasegawa-Johnson, and D. Cox. Unsupervised speech decomposition via triple information bottleneck. In *ICML*, volume 119, pages 7836–7846, 2020.
- [29] K. Qian, Y. Zhang, S. Chang, X. Yang, and M. Hasegawa-Johnson. AutoVC: Zero-shot voice style transfer with only autoencoder loss. In *ICML*, volume 97, pages 5210–5219, 2019.
- [30] M. V. Ramos. Voice conversion with deep learning. Master’s thesis, Instituto Superior Técnico, 2016.
- [31] C. Robinson, N. Obin, and A. Roebel. Sequence-to-sequence modelling of F0 for speech emotion conversion. In *ICASSP*, pages 6830–6834, 2019.
- [32] T. Salimans and D. P. Kingma. Weight normalization: A simple reparameterization to accelerate training of deep neural networks. In *NeurIPS*, volume 29, pages 901–909, 2016.
- [33] M. Sambur. Selection of acoustic features for speaker identification. *IEEE Transactions on Signal Processing*, 23(2):176–182, 1975.
- [34] J. Serrà, S. Pascual, and C. S. Perales. Blow: a single-scale hyperconditioned flow for non-parallel raw-audio voice conversion. In *NeurIPS*, volume 32, pages 6793–6803, 2019.
- [35] Y. Stylianou, O. Cappe, and E. Moulines. Continuous probabilistic transform for voice conversion. *TASLP*, 6(2):131–142, 1998.
- [36] L. Sun, K. Li, H. Wang, S. Kang, and H. Meng. Phonetic posteriorgrams for many-to-one voice conversion without parallel data training. In *ICME*, pages 1–6, 2016.
- [37] A. Tamamori, T. Hayashi, K. Kobayashi, K. Takeda, and T. Toda. Speaker-dependent WaveNet vocoder. In *Interspeech*, pages 1118–1122, 2017.

- [38] T. Toda, A. W. Black, and K. Tokuda. Voice conversion based on maximum-likelihood estimation of spectral parameter trajectory. *TASLP*, 15(8):2222–2235, 2007.
- [39] A. van den Oord, O. Vinyals, and K. Kavukcuoglu. Neural discrete representation learning. In *NeurIPS*, volume 30, pages 6309–6318, 2017.
- [40] R. Yamamoto, E. Song, and J.-M. Kim. Parallel WaveGAN: A fast waveform generation model based on generative adversarial networks with multi-resolution spectrogram. In *ICASSP*, pages 6199–6203, 2020.
- [41] J.-X. Zhang, Z.-H. Ling, L.-J. Liu, Y. Jiang, and L.-R. Dai. Voice conversion based on maximum-likelihood estimation of spectral parameter trajectory. *TASLP*, 27(3):631–644, 2019.